Towards the Heisenberg limit in microwave photon detection by a qubit array

P. Navez ⬤, A. G. Balanov ⬤, S. E. Savel'ev ⬤, and A. M. Zagoskin ⬤

Department of Physics, Loughborough University, Loughborough LE11 3TU, United Kingdom

Using an analytically solvable model, we show that a qubit array-based detector allows one to achieve the fundamental Heisenberg limit in detecting single photons. In the case of superconducting qubits, this opens other opportunities for quantum sensing and communications in the important microwave range.

I. INTRODUCTION

Single photon detection has been initiated in the optical regime, but is now being actively pursued in the microwave range. Its motivations come from different fields, ranging from quantum communications [1], sensing [2], and medical imaging [3], to the search for axions, hypothetical ingredients of dark matter [4–6] (an axion in a magnetic field would convert to a single microwave photon).

The natural frequency range of superconducting qubits is in the microwave regime [7], which facilitates their use for detection of single microwave photons [8–11]. Still, it remains a challenging task, in particular because of the significant level of ambient noise in this frequency range.

The fast progress in the quality and complexity of experimentally realized superconducting qubit arrays coupled to waveguides [12–17] as well as in the theory of these quantum metamaterials [18–22] stimulated the inquiry into the practical possibility of their application to single photon detection. It was shown [23] that for an array of $\mathcal{N}$ uncorrelated, noninteracting qubits used for a quantum nondemolition detection of a photon, the signal-to-noise ratio (SNR) ratio grows as $\sqrt{\mathcal{N}}$, corresponding to the standard standard quantum limit (SQL), and it was suggested [24] that introducing some specific quantum correlations could realize the so-called Heisenberg limit for SNR, i.e., to have SNR scaling as $\mathcal{N}$ rather than $\sqrt{\mathcal{N}}$.

Essentially, SQL is not *the* fundamental limit on the accuracy achieved by $\mathcal{N}$ measurements of the system (in parallel or consecutively). It applies to the case of independent inputs and is the consequence of the central limit theorem [25]. If the inputs are properly quantum correlated, then the accuracy is proportional to $1/\mathcal{N}$ rather than $1/\sqrt{\mathcal{N}}$, and this is the best possible outcome [24]. Remarkably, achieving the Heisenberg limit does not depend on whether the *measurements* are quantum correlated; it is only the quantum correlations between the *inputs* that count [24].

Several possible implementations for achieving the Heisenberg limit had been suggested [24], but its experimental realization remains a challenging task, especially outside the optical range. In this paper we show that the Heisenberg limit for SNR can be achieved in principle using the quantum non-demolition measurement of an array of qubits, which plays the role of an antenna. This result may be of particular importance for superconducting qubit arrays, which would be a natural choice for the detection of single microwave photons [23]. For convenience and without the loss of generality, we are using the language appropriate for this particular realization of the proposed approach. In Sec. II, we formulate an exactly solvable model Hamiltonian in the presence of a thermal noise and, in Sec. III, we analyze the obtained results according to the level of input correlations between the qubits.

II. EXACTLY SOLVABLE MODEL

A. Model Hamiltonian

Without loss of generality, we start from the scheme presented in Fig. 1. There are N identical waveguides indexed by $\nu = 1, 2, \ldots, N$, each containing M identical qubits and $\mu = 1, 2, \ldots, M$. These qubits are prepared either in a factorized superposition state $|\Psi_F\rangle = \prod_{\nu,\mu} |\psi\rangle_{\nu,\mu} = \prod(|0\rangle_{\nu,\mu} + |1\rangle_{\nu,\mu})/\sqrt{2}$, or in a more complicated entangled state chosen to maximize the SNR.

An input signal consists of n photons ($n = 0, 1$) and is uniformly fed into the same mode of waveguides. As in Ref. [23], the qubits are detuned from the mode frequency (dispersive regime) to ensure that there is no absorption. Thus the qubit-field interaction is a quantum nondemolition kind of process.

The annihilation operator for the input signal $\hat{a}$ can be then written as

$$\hat{a} = \sum_{\nu=1}^{N} \frac{1}{\sqrt{N}} \hat{a}_\nu. \tag{1}$$

Here, $\hat{a}_\nu$ describes the submode, which travels in the waveguide ν. The qubit is described by Pauli matrices $\hat{\sigma}_{\nu,\mu}^x = |1\rangle_{\nu,\mu}\langle 0| + |0\rangle_{\nu,\mu}\langle 1|$, $\hat{\sigma}_{\nu,\mu}^y = -i|1\rangle_{\nu,\mu}\langle 0| + i|0\rangle_{\nu,\mu}\langle 1|$, and $\hat{\sigma}_{\nu,\mu}^z = |1\rangle_{\nu,\mu}\langle 1| - |0\rangle_{\nu,\mu}\langle 0|$. The rising/lowering operators are $\hat{\sigma}_{\nu,\mu}^{\pm} = (\hat{\sigma}_{\nu,\mu}^x \pm i\hat{\sigma}_{\nu,\mu}^y)/2$.

Even in the absence of a direct qubit-qubit interaction, they will interact through the virtual excitations of the vacuum waveguide mode, which in the case of a large number of
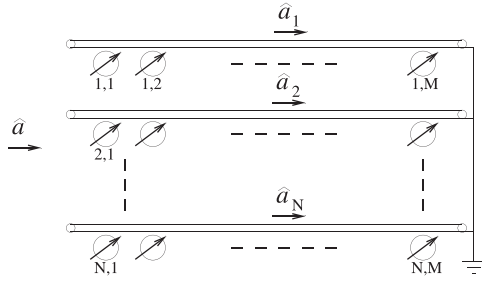
FIG. 1. Schematic representation of the single photon detector. The signal propagates horizontally through N parallel waveguides, each containing M qubits.

qubits can be approximated by the mean-field term in the Hamiltonian proportional to $h_\delta \hat{\sigma}^x_{\nu,\mu}$ [23]. During the relevant time interval τ_1 this interaction induces a rotation of the qubit state about $0x$ by an angle $\Delta = \tau_1 h_\delta \ll 1$. The interaction of qubits with the photon field in the dispersive regime is given by a term $\propto h_p \hat{a}^\dagger_\nu \hat{a}_\nu \hat{\sigma}^z_{\nu,\mu}$. When one photon passes by a qubit (with an effective interaction time τ_2), it will induce a qubit state rotation about the $0z$ axis by $\theta = \tau_2 h_p$. If the distance between the qubits is much smaller than the photon wavelength, we can assume that the interaction with all qubits is simultaneous. In the absence of noise, the time-dependent Hamiltonian can be thus written as

$$
\hat{H}(t) = -\left[\sum_{\nu,\mu=1}^{N,M} R\left(\frac{t}{\tau_1} - \frac{1}{2}\right) \frac{h_\delta}{2} \hat{\sigma}^x_{\nu,\mu} \right.
$$
$$
\left. + R\left(\frac{t-\tau_1}{\tau_2} - \frac{1}{2}\right) \frac{h_p}{2} \hat{\sigma}^z_{\nu,\mu} \hat{a}^\dagger_\nu \hat{a}_\nu \right], \quad (2)
$$

where we use the rectangular window function

$$
R(t) = \begin{cases} 0, & \text{if } |t| > \frac{1}{2}, \\ \frac{1}{2}, & \text{if } |t| = \frac{1}{2}, \\ 1, & \text{if } |t| < \frac{1}{2}. \end{cases} \quad (3)
$$

B. Noise

We consider the simultaneous action of kinds of noise. The first kind is inherent in the quantum state chosen to describe the qubit ensemble. The readout measurement has an intrinsic shot noise from uncorrelated qubits that is probed from the quantum fluctuations of the spin operators. We expect that an adequate quantum entanglement would correlate the qubit states and decrease this measurement noise.

The second kind of noise originates from the imperfect transmission of the signal to the qubits and leads to the dephasing. It may be caused by imperfections of the waveguide, thermal photons inside the cavity or in the qubits, or other sources of ambient noise. It is modeled by the additional quantum noise field $\hat{b}_{\nu,\mu}$ that reduces the quantum efficiency $\eta < 1$. As a result, the actual signal interacting with the qubit (ν, μ) will be

$$
\hat{a}'_{\nu,\mu} = \sqrt{\eta}\hat{a}_\nu + \sqrt{1-\eta}\hat{b}_{\nu,\mu}. \quad (4)
$$

For a thermal noise field, the disturbance will depend on the effective noise temperature T. Note that this effect accounts

also for the backscattering field,

$$
\hat{b}'_{\nu,\mu} = -\sqrt{1-\eta}\hat{a}_\nu + \sqrt{\eta}\hat{b}_{\nu,\mu}. \quad (5)
$$

We express the noise through its Fourier components $\hat{b}_{\nu,k_z}$ inside each waveguide,

$$
\hat{b}_{\nu,\mu} = \sum_{\mu=1}^{M} \frac{e^{2\pi i k_z \mu/M}}{\sqrt{M}} \hat{b}_{\nu,k_z}. \quad (6)
$$

These evolve with the dispersion relation frequency ω_{k_z}. Therefore

$$
\hat{a}'_{\nu,k_z} = \sqrt{\eta}\hat{a}_\nu + \sqrt{1-\eta}\hat{b}_{\nu,k_z}. \quad (7)
$$

With all these contributions, the initial quantum state has many degrees of freedom. Modeling the noise in the waveguide by a blackbody radiation, we have for the initial density matrix of the system the following expression:

$$
\hat{\rho}_n = \frac{\exp\left(-\sum_{\nu,k_z=1}^{N,M} \frac{\hbar\omega_{k_z}}{k_B T} \hat{b}^\dagger_{\nu,k_z} \hat{b}_{\nu,k_z}\right)}{\text{Tr}\left[\exp\left(-\sum_{\nu,k_z=1}^{N,M} \frac{\hbar\omega_{k_z}}{k_B T} \hat{b}^\dagger_{\nu,k_z} \hat{b}_{\nu,k_z}\right)\right]} |n\rangle\langle n| |\Psi\rangle\langle\Psi|. \quad (8)
$$

Here, $|n\rangle = (1/\sqrt{n!})\left[\frac{\sum_{\nu=1}^{N}\hat{a}^\dagger_\nu}{\sqrt{N}}\right]^n |0\rangle$ is the state of the signal photon field with $n(=0, 1)$ photons, and $|\Psi\rangle$ is the quantum state of the qubits.

The other sources of noise are the relaxation of the qubits and the effects of finite preparation and readout timescales. We have described by a single effective decay rate Γ. It affects the initial state since the qubit readout is delayed by the finite time interval $\tau_1 + \tau_2$ during the photon passage. If no photon passes through the line, the quantum state becomes mixed with the density matrix:

$$
|\psi\rangle_{\nu,\mu}\langle\psi| \rightarrow \hat{\rho}_{\nu,\mu}(t)
$$
$$
= \frac{1}{2}\left\{\exp(-\Gamma t)\hat{\sigma}^x_{\nu,\mu} + [\exp(-2\Gamma t) - 1]\hat{\sigma}^z_{\nu,\mu} + \hat{1}\right\}. \quad (9)
$$

Therefore, we must ensure that the photon passage time should be short enough, so that $\tau_1 + \tau_2 \ll 1/\Gamma$ (see also Refs. [26,27]). This condition can be fulfilled since the decay rate is in the MHz range in comparison to the photon frequency in the GHz range. The addition of direct qubit-qubit coupling generates an entangled ground state, stabilizes the initial state $|\Psi_F\rangle$, and suppresses the relaxation rate (see Sec. III B).

C. System evolution

In the Heisenberg representation, the two successive qubit rotations (by an angle Δ during the time τ_1 due to effective qubit-qubit interactions, and by an angle θ during the time τ_2 due to direct qubit-photon interaction) produce a unitary transformation of field operators. For the qubit, we obtain after the total time $\tau_1 + \tau_2$ the new "spin" operators:

$$
\hat{\sigma}'^i_{\nu,\mu} = \hat{U}_\sigma \hat{\sigma}^i_{\nu,\mu} \hat{U}^\dagger_\sigma, \quad i = (x, y, z), \quad (10)
$$

$$
\hat{U}_\sigma = \prod_{\nu,\mu=1}^{N,M} \exp\left(-i\frac{\theta}{2}\hat{a}'^\dagger_{\nu,\mu}\hat{a}'_{\nu,\mu}\hat{\sigma}^z_{\nu,\mu}\right) \exp\left(-i\frac{\Delta}{2}\hat{\sigma}^x_{\nu,\mu}\right). \quad (11)
$$

Using the operator algebra, we bring these expressions to a simpler form,

$$\hat{\sigma}'^z_{\nu,\mu} = \cos(\Delta)\hat{\sigma}^z_{\nu,\mu} - \sin(\Delta)\cos(\theta\hat{a}'^\dagger_{\nu,\mu}\hat{a}'_{\nu,\mu})\hat{\sigma}^y_{\nu,\mu}$$
$$+ \sin(\Delta)\sin(\theta\hat{a}'^\dagger_{\nu,\mu}\hat{a}'_{\nu,\mu})\hat{\sigma}^x_{\nu,\mu}. \quad (12)$$

It remains to determine the expectation values of these operators for various qubit configurations using the definition $\langle\hat{\mathcal{O}}\rangle = \mathrm{tr}(\hat{\rho}_n\hat{\mathcal{O}})$.

III. RESULTS

A. Uncorrelated initial qubit state

The simplest qubit configuration is the factorized state given by $|\Psi_F\rangle = \prod_{\nu,\mu=1}^{N,M}(|0\rangle_{\nu,\mu} + |1\rangle_{\nu,\mu})/\sqrt{2}$. Using Eqs. (12) and observing that the signal affects equally each qubit, we obtain for the average magnetic flux of the array

$$\langle\hat{S}'^z\rangle = \sum_{\nu,\mu=1}^{N,M}\frac{\langle\hat{\sigma}'^z_{\nu,\mu}\rangle}{2} = \frac{NM}{2}\sin(\Delta)\langle\sin(\theta\hat{a}'^\dagger_{\nu,\mu}\hat{a}'_{\nu,\mu})\rangle. \quad (13)$$

Quite generally, we obtain for the detection of n photons (see the Appendix)

$$\langle\sin(\theta\hat{a}'^\dagger_{\nu,\mu}\hat{a}'_{\nu,\mu})\rangle_n$$
$$= \frac{-i/2}{1 + f_T(1 - e^{i\theta})}\left[1 + \frac{\eta(e^{i\theta} - 1)}{N[1 + f_T(1 - e^{i\theta})]}\right]^n + \mathrm{c.c.}, \quad (14)$$

where $f_T = (1 - \eta)\overline{f}$ is the fraction of thermal noise deteriorating the signal, $\overline{f} = \sum_{k_z=1}^M f_{k_z}/M$ is the noise density, and $f_{k_z} = 1/[\exp(\hbar\omega_{k_z}/k_BT) - 1]$ is the Bose-Einstein factor. In particular, we find for $n = 0, 1$,

$$\langle\sin(\theta\hat{a}'^\dagger_{\nu,\mu}\hat{a}'_{\nu,\mu})\rangle_0$$
$$= \frac{f_T\sin\theta}{[1 + f_T(1 - \cos\theta)]^2 + f_T^2\sin^2\theta}, \quad (15)$$
$$\langle\sin(\theta\hat{a}'^\dagger_{\nu,\mu}\hat{a}'_{\nu,\mu})\rangle_1$$
$$= \langle\sin(\theta\hat{a}'^\dagger_{\nu,\mu}\hat{a}'_{\nu,\mu})\rangle_0$$
$$+ \frac{\eta\sin\theta[1 - 2(1 - \cos\theta)f_T^2]}{N\{[1 + f_T(1 - \cos\theta)]^2 + f_T^2\sin^2\theta\}^2}. \quad (16)$$

For small Δ, we deduce also that the fluctuations scale normally as NM since

$$\langle\delta^2\hat{S}'^z\rangle = NM/4 + \mathcal{O}(\Delta). \quad (17)$$

Thus, the SNR for an n-photon detection is defined as

$$SNR_n = \frac{\langle\hat{S}'^z\rangle}{\sqrt{\langle\delta^2\hat{S}'^z\rangle}} = R\sqrt{N}\Delta\langle\sin(\theta\hat{a}'^\dagger_{\nu,\mu}\hat{a}'_{\nu,\mu})\rangle_n, \quad (18)$$

where $R = \sqrt{M}$ corresponds to the standard quantum limit. This last result implies that, as a function of N, SNR scales as $\sqrt{N}$ for small Δ in the absence of a photon but becomes worse in the presence of one photon. However, as a function of M, the scaling is always $\sqrt{M}$ irrelevant of the number of photons
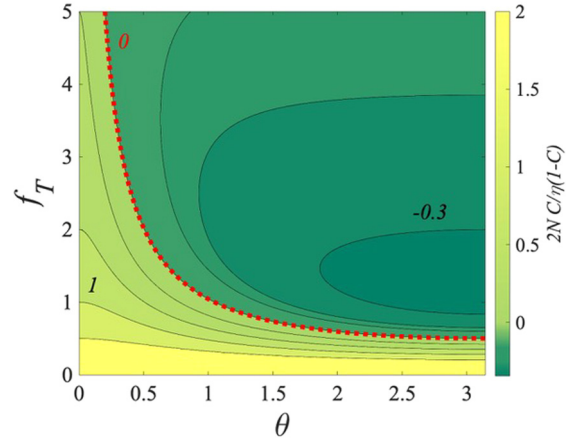

FIG. 2. Plot of the renormalized contrast vs the angle shift θ and the thermal noise intensity f_T.

detected. This observation indicates that $N = 1$ is the optimal value for a single photon detection.

The contrast is defined as

$$\mathcal{C} \equiv \frac{\langle\sin(\theta\hat{a}'^\dagger_{\nu,\mu}\hat{a}'_{\nu,\mu})\rangle_1 - \langle\sin(\theta\hat{a}'^\dagger_{\nu,\mu}\hat{a}'_{\nu,\mu})\rangle_0}{\langle\sin(\theta\hat{a}'^\dagger_{\nu,\mu}\hat{a}'_{\nu,\mu})\rangle_0 + \langle\sin(\theta\hat{a}'^\dagger_{\nu,\mu}\hat{a}'_{\nu,\mu})\rangle_1}. \quad (19)$$

This expression can be reduced to

$$\frac{N}{\eta}\frac{2\mathcal{C}}{1 - \mathcal{C}} = \frac{1 - 2(1 - \cos\theta)f_T^2}{f_T[1 + 2(1 - \cos\theta)(f_T + f_T^2)]}. \quad (20)$$

The left-hand side reflects the contrast normalized by the quantum efficiency and N, whose dependence on angle shift and thermal noise fraction is presented in Fig. 2. As expected, the contrast decreases when the noise density increases, but this effect is more important for large rotation angles θ. It shows a regime of negative contrast when the noise density exceeds the critical value $f_T > 1/\sqrt{2(1 - \cos\theta)}$. For rather small noise, $f_T < 0.5$, the contrast is positive for any $\theta \in (0, \pi)$. With this, $C > 0$ for any finite f_T if the qubit-photon interaction does not cause much qubit rotation, i.e., for vanishing θ.

B. Perfectly correlated state

Correlated states involving qubits with equal ν but different μ improve the signal-to-noise ratio. More precisely, using the notation $\hat{S}^i_\nu = \sum_{\mu=1}^M\hat{\sigma}^i_{\nu,\mu}/2$, we notice from (18) that SNR for small Δ is proportional to $R = \langle\hat{S}^x_\nu\rangle/\langle\hat{S}^{z\,2}_\nu\rangle^{1/2}$, which is equal to $\sqrt{M}$ in the uncorrelated case. This observation suggests that the optimal state is the one that maximizes R and therefore is the ground state of the quantum Ising Hamiltonian with a strong qubit-qubit coupling,

$$\hat{H}_\nu = \hat{S}^{z\,2}_\nu + \lambda\hat{S}^x_\nu. \quad (21)$$

The coefficient λ is the Lagrange multiplier that controls the necessary level of correlation. It should be small since an optimal result is obtained for strong quantum correlations. It is worth pointing out this connection between the magnetometry quantum sensing in cold atoms and the single photon detection using qubit detection. The optimization of SNR amounts to

obtaining the highest possible spin squeezing [28]. Then we may use the perturbation theory. In the zeroth order ($\lambda \to 0$), we start from the total angular momentum state $|l, m\rangle_\nu$ as the eigenstate of $\hat{\mathbf{S}}_\nu^2 = \sum_{i=x,y,z} \hat{S}_\nu^{i\,2}$ and $\hat{S}_\nu^z$ with eigenvalues $l(l+1)$ and m, respectively, and where we identify $l = M/2$. The ground state combines states of m very close to zero and thus corresponds to a giant spin state that entangles all the individual qubits.

In the next order, there are two cases:

M odd. The next order is a linear combination of the two degenerate ground states $|M/2, \pm 1/2\rangle_\nu$. We find the correlated state $|\Psi\rangle = \prod_{\nu=1}^{N}(|M/2, 1/2\rangle_\nu + |M/2, -1/2\rangle_\nu)/\sqrt{2}$ that corresponds to a maximally entangled state. We determine that $\langle \delta^2 \hat{S}_\nu^z \rangle = 1/4$ is independent on M and that $\langle \hat{S}_\nu^x \rangle = (M+1)/4$. We find therefore $R = (M+1)/2$ which corresponds asymptotically to the Heisenberg limit.

M even. The ground state for $\lambda = 0$ corresponds to a maximally entangled state of individual qubits,

$$|M/2, 0\rangle_\nu = \frac{(M/2)!}{\sqrt{M!}} \sum_{\substack{s_\mu = \pm 1/2 \\ \sum_{\mu=1}^{M} s_\mu = 0}} |s_1, \ldots, s_\mu, \ldots, s_M\rangle_\nu, \quad (22)$$

with spin s_μ along the z axis. Each individual state is also an eigenstate for $\lambda = 0$.

The expansion to the second order involves the entangled combination $|\Psi\rangle = \prod_{\nu=1}^{N} \sum_{m=-1}^{1} \alpha_m |M/2, m\rangle_\nu$. We determine $\langle \delta^2 \hat{S}_\nu^z \rangle = \lambda^2 (M/2+1)M/4$ and $\langle \hat{S}_\nu^x \rangle = \lambda(M/2+1)M/2$. We find therefore $R = \sqrt{M(M/2+1)}$, which also asymptotically tends to the Heisenberg limit which agrees with the results for squeezed spin states in Ref. [29].

Such a maximally correlated state of the qubit set, which imposes the maximal rigidity on it producing a "giant spin," is not realistic from the experimental point of view. Generally, restrictions imposed by the qubit circuit geometry limit their connectivity or couplings to the architecture in clusters. A relaxation of effective qubit-qubit coupling affects the rigidity and deteriorates the SNR. Indeed, the introduction of a perturbation additional small term (which softens the "giant spin")

$$\hat{H}_\nu' = \sum_{\mu \neq \mu'=1}^{M} p_{\mu\mu'} \frac{\hat{\sigma}_{\nu,\mu}^z \hat{\sigma}_{\nu,\mu'}^z}{4} \quad (23)$$

raises the degeneracy of the individual states. Assume a simplified case where there is interaction between $M - M_E$ spins, while other M_E spins do not interact. For M_E even, the state that minimizes the perturbation Hamiltonian for $\lambda = 0$ can be decomposed into an uncorrelated state of $M - M_E$ spins and a perfectly correlated state of M_E spins described by an angular state with angular momentum number $M_E/2$ written as

$$|\Psi\rangle_\nu = |\pm s_1, \ldots, \pm s_{M-M_E}\rangle |M_E/2, 0\rangle_\nu. \quad (24)$$

In this expression, there are two possible degenerate states of opposite uncorrelated spins. Again, as the result of second-order perturbation theory, we obtain the expression for R,

$$R = \sqrt{M_E(M_E/2+1) + M - M_E}, \quad (25)$$

which interpolates between the uncorrelated regime and the Heisenberg regime. Figure 3 shows the increase of the SNR
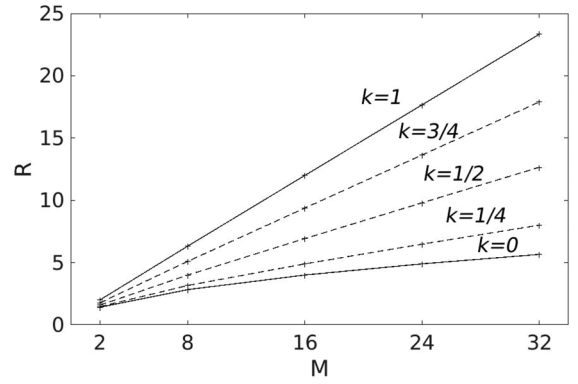

FIG. 3. Signal-to-noise ratio R vs qubit number M for a perfect correlated state ($k = 1$), noncorrelated state ($k = 0$), and intermediate regimes ($0 < k < 1$).

with the qubit number M for various entanglement states characterized by the ratio $k = M_E/M$. This last result illustrates that the Heisenberg limit of SNR is not fragile with respect to perturbations.

M = 2 for any λ. For this simpler situation, exact diagonalization is possible. Using the correlated state $|\Psi\rangle = \prod_{\nu=1}^{N} \sum_{m=-1}^{1} \alpha_m |M/2, m\rangle_\nu$, we determine the coefficient α_m and find the ratio

$$R = \sqrt{2 + \frac{2}{\sqrt{1+4\lambda^2}}}. \quad (26)$$

Thus λ controls the crossover from an uncorrelated state ($R = \sqrt{2}$ at $\lambda = \infty$) to a fully correlated or entangled state ($R = 2$ at $\lambda = 0$), with the corresponding transition from the SQL to the Heisenberg limit.

C. Nearest-neighbor interacting state

Since the qubits are placed in a linear chain along the waveguide, we can use the quantum Ising Hamiltonian with only nearest-neighbor coupling,

$$\hat{H}_\nu = \sum_{\mu=1}^{M} \frac{\hat{\sigma}_{\nu,\mu+1}^z \hat{\sigma}_{\nu,\mu}^z}{2} + \lambda \frac{\hat{\sigma}_{\nu,\mu}^x}{2}, \quad (27)$$

where we use the periodic boundary condition for simplicity ($\hat{\sigma}_{\nu,M+1}^z = \hat{\sigma}_{\nu,1}^z$).

We define the antiferromagnetic state $|AF\rangle_\nu$ as the ground state for $\lambda = 0$. These are two such degenerate states but we will only consider one since they are separated by a large potential barrier for large N. In the case of $\lambda \to 0$, we use again the second-order perturbation theory with the correlated state $|\Psi\rangle = \prod_{\nu=1}^{N}(\alpha_0 + \alpha_1 \hat{S}_\nu^+ + \alpha_{-1} \hat{S}_\nu^-)|AF\rangle_\nu$. There are again two cases:

M even. We find $\langle \delta^2 \hat{S}_\nu^z \rangle = \lambda^2 M/16$ and $\langle \hat{S}_\nu^x \rangle = \lambda M/4$. Therefore we find no improvement since $R = \sqrt{M}$ is left unchanged.

M odd. We find for large M that $\langle \delta^2 \hat{S}_\nu^z \rangle = (1 + \lambda^2 M/4)/4$ and $\langle \hat{S}_\nu^x \rangle = \lambda M/4$. We find therefore $R = \lambda M/\sqrt{4 + \lambda^2 M} \to \sqrt{M}$ for large M. In the limit of small λ, however, we find $R = \lambda M/2$, which is again the Heisenberg limit, but only achieved for $\lambda \ll 1$.

Therefore the nearest-neighbor coupling is useless if the goal is to reach the Heisenberg limit of the signal-to-noise ratio in a quantum detector array.

IV. CONCLUSION

We have analyzed a detector consisting of an array of qubits in the presence of noise and interaction. Using an exactly solvable model, we have shown that quantum correlations of the state of array allow one to reach the Heisenberg limit, that is, increase the signal-to-noise ratio proportionally to the total number of qubits (forming together the detected signal) rather than its square root. The rigidity of the qubit system is the crucial requirement for achieving this effect, which makes connectivity between qubits in a detector array the key parameter in designing similar systems. Our findings provide an important insight for the strategy of reaching the Heisenberg limit, in the design of efficient qubit-based quantum detectors.

In our generic model we have neglected the size of the qubits compared to the microwave wavelength. We also do not specify the origin of the interaction, which produces the interqubit coupling. A natural extension of this study will be the investigation of different geometries of qubit arrays and of the effects of specifics of the interqubit interaction (dipole-dipole, inductive, etc.).

APPENDIX

The expectation value of the phase is determined using the coherent state formalism. Defining the coherent state $|\alpha\rangle_\nu = \sum_{n=0}^{\infty} e^{-|\alpha|^2/2}\alpha^n(\hat{a}_\nu^\dagger)^n|0\rangle_\nu/n!$ and $|\beta\rangle_{\nu,\mu} = \sum_{n=0}^{\infty} e^{-|\beta|^2/2}\beta^n(\hat{b}_{\nu,\mu}^\dagger)^n|0\rangle_{\nu,\mu}/n!$, we can calculate successively the coherent state average:

$$
\begin{aligned}
{}_\nu\langle\alpha|_{\nu,\mu}\langle\beta|\exp[i\theta\hat{a}_{\nu,\mu}^{\prime\dagger}\hat{a}_{\nu,\mu}']|\alpha\rangle_\nu|\beta\rangle_{\nu,\mu} &= {}_\nu\langle\alpha|_{\nu,\mu}\langle\beta|\exp[i\theta(\sqrt{\eta}\hat{a}_\nu^\dagger + \sqrt{1-\eta}\hat{b}_{\nu,\mu}^\dagger)(\sqrt{\eta}\hat{a}_\nu + \sqrt{1-\eta}\hat{b}_{\nu,\mu})]|\alpha\rangle_\nu|\beta\rangle_{\nu,\mu} \\
&= {}_\nu\langle 0|_{\nu,\mu}\langle 0|\exp[i\theta(\hat{a}_{\nu,\mu}^{\prime\dagger} + \sqrt{\eta}\alpha^* + \sqrt{1-\eta}\beta^*)(\hat{a}_{\nu,\mu}' + \sqrt{\eta}\alpha + \sqrt{1-\eta}\beta)]|0\rangle_\nu|0\rangle_{\nu,\mu} \\
&= {}_{\nu,\mu}\langle\sqrt{\eta}\alpha + \sqrt{1-\eta}\beta|\exp[i\theta\hat{a}_{\nu,\mu}^{\prime\dagger}\hat{a}_{\nu,\mu}']|\sqrt{\eta}\alpha + \sqrt{1-\eta}\beta\rangle_{\nu,\mu} \\
&= {}_{\nu,\mu}\langle\sqrt{\eta}\alpha + \sqrt{1-\eta}\beta|e^{i\theta}(\sqrt{\eta}\alpha + \sqrt{1-\eta}\beta)\rangle_{\nu,\mu} \\
&= \exp[(e^{i\theta}-1)|\sqrt{\eta}\alpha + \sqrt{1-\eta}\beta|^2].
\end{aligned}
\tag{A1}
$$

The thermal state caused by the noise is related to the coherent state through the formula

$$
\frac{\exp\left(-\hbar\omega_{k_z}\hat{b}_{\nu,k_z}^\dagger\hat{b}_{\nu,k_z}/k_BT\right)}{\mathrm{Tr}\left[\exp\left(-\hbar\omega_{k_z}\hat{b}_{\nu,k_z}^\dagger\hat{b}_{\nu,k_z}/k_BT\right)\right]} = \int\frac{d^2\beta}{\pi f_{k_z}}\exp\left(-|\beta|^2/f_{k_z}\right)|\beta\rangle_{\nu,k_z}\langle\beta|.
\tag{A2}
$$

With this procedure, we obtain an expression for the thermal average:

$$
\begin{aligned}
&\mathrm{Tr}\left[|\alpha\rangle_\nu\langle\alpha|\frac{\exp\left(-\sum_{k_z=1}^{M}\hbar\omega_{k_z}\hat{b}_{\nu,k_z}^\dagger\hat{b}_{\nu,k_z}/k_BT\right)}{\mathrm{Tr}\left[\exp\left(-\sum_{k_z=1}^{M}\hbar\omega_{k_z}\hat{b}_{\nu,k_z}^\dagger\hat{b}_{\nu,k_z}/k_BT\right)\right]}\exp[i\theta\hat{a}_{\nu,\mu}^{\prime\dagger}\hat{a}_{\nu,\mu}']\right] \\
&= \prod_{k_z=1}^{M}\int\frac{d^2\beta_{k_z}}{\pi f_{k_z}}\exp\left(-|\beta_{k_z}|^2/f_{k_z}\right)\exp\left[(e^{i\theta}-1)\left|\sqrt{\eta}\alpha + \sqrt{1-\eta}\sum_{k_z=1}^{M}\frac{\exp(i2\pi k_z\nu/M)}{\sqrt{M}}\beta_{k_z}\right|^2\right] \\
&= \frac{1}{1+f_T(1-e^{i\theta})}\exp\left[\frac{\eta(e^{i\theta}-1)|\alpha|^2}{1+f_T(1-e^{i\theta})}\right].
\end{aligned}
\tag{A3}
$$

It remains to generalize the expressions for N channels and carry out an expansion development in the photon number. Using the property that $|\alpha\rangle = \prod_{\nu=1}^{N}|\alpha/\sqrt{N}\rangle_\nu$, we determine

$$
\begin{aligned}
\langle\exp[i\theta\hat{a}_{\nu,\mu}^{\prime\dagger}\hat{a}_{\nu,\mu}']\rangle &= \mathrm{Tr}\left[|\alpha\rangle\langle\alpha|\frac{\exp\left(-\sum_{\nu',k_z=1}^{N,M}\hbar\omega_{k_z}\hat{b}_{\nu',k_z}^\dagger\hat{b}_{\nu',k_z}/k_BT\right)}{\mathrm{Tr}\left[\exp\left(-\sum_{\nu',k_z=1}^{N,M}\hbar\omega_{k_z}\hat{b}_{\nu',k_z}^\dagger\hat{b}_{\nu',k_z}/k_BT\right)\right]}\exp[i\theta\hat{a}_{\nu,\mu}^{\prime\dagger}\hat{a}_{\nu,\mu}']\right] \\
&= \frac{1}{1+f_T(1-e^{i\theta})}\exp\left[\frac{\eta(e^{i\theta}-1)|\alpha|^2}{N[1+f_T(1-e^{i\theta})]}\right].
\end{aligned}
\tag{A4}
$$

Finally, by an expansion in α, we deduce the average for the case of n photons:

$$\langle \exp[i\theta \hat{a}'^{\dagger}_{\nu,\mu} \hat{a}'_{\nu,\mu}] \rangle_n = \text{Tr} \left[|n\rangle\langle n| \frac{\exp\left(-\sum_{\nu',k_z=1}^{N,M} \hbar\omega_{k_z} \hat{b}^{\dagger}_{\nu',k_z} \hat{b}_{\nu',k_z}/k_B T\right)}{\text{Tr}\left[\exp\left(-\sum_{\nu',k_z=1}^{N,M} \hbar\omega_{k_z} \hat{b}^{\dagger}_{\nu',k_z} \hat{b}_{\nu',k_z}/k_B T\right)\right]} \exp[i\theta \hat{a}'^{\dagger}_{\nu,\mu} \hat{a}'_{\nu,\mu}] \right]$$

$$= \frac{1}{1 + f_T(1 - e^{i\theta})} \left[1 + \frac{\eta(e^{i\theta} - 1)}{N[1 + f_T(1 - e^{i\theta})]} \right]^n. \tag{A5}$$

[1] J.-G. Ren, P. Xu, H.-L. Yong, L. Zhang, S.-K. Liao, J. Yin, W.-Y. Liu, W.-Q. Cai, M. Yang, M. Li *et al.*, Nature (London) **549**, 70 (2017).

[2] R. Santagati, A. A. Gentile, S. Knauer, S. Schmitt, S. Paesani, C. Granade, N. Wiebe, C. Osterkamp, L. P. McGuinness, J. Wang, M. G. Thompson, J. G. Rarity, F. Jelezko, and A. Laing, Phys. Rev. X **9**, 021019 (2019).

[3] B. T. Kiani, A. Villanyi, and S. Lloyd, arXiv:2004.02036.

[4] L. D. Duffy and K. van Bibber, New J. Phys. **11**, 105008 (2009).

[5] C. Beck, Phys. Dark Universe **7-8**, 6 (2015).

[6] A. V. Dixit, S. Chakram, K. He, A. Agrawal, R. K. Naik, D. I. Schuster, and A. Chou, arXiv:2008.12231.

[7] A. M. Zagoskin, *Quantum Engineering: Theory and Design of Quantum Coherent Structures* (Cambridge University Press, Cambridge, UK, 2011).

[8] D. I. Schuster, A. A. Houck, J. A. Schreier, A. Wallraff, J. M. Gambetta, A. Blais, L. Frunzio, J. Majer, B. Johnson, M. H. Devoret, S. M. Girvin, and R. J. Schoelkopf, Nature (London) **445**, 515 (2007).

[9] K. Inomata, Z. Lin, K. Koshino, W. D. Oliver, J.-S. Tsai, T. Yamamoto, and Y. Nakamura, Nat. Commun. **7**, 12303 (2016).

[10] X. Gu, A. F. Kockum, A. Miranowicz, Y.-xi Liu, and F. Nori, Phys. Rep. **718-719**, 1 (2017).

[11] S. R. Sathyamoorthy, L. Tornberg, A. F. Kockum, B. Q. Baragiola, J. Combes, C. M. Wilson, T. M. Stace, and G. Johansson, Phys. Rev. Lett. **112**, 093601 (2014).

[12] H. Paik, D. I. Schuster, L. S. Bishop, G. Kirchmair, G. Catelani, A. P. Sears, B. R. Johnson, M. J. Reagor, L. Frunzio, L. I. Glazman, S. M. Girvin, M. H. Devoret, and R. J. Schoelkopf, Phys. Rev. Lett. **107**, 240501 (2011).

[13] J. Koch, T. M. Yu, J. Gambetta, A. A. Houck, D. I. Schuster, J. Majer, A. Blais, M. H. Devoret, S. M. Girvin, and R. J. Schoelkopf, Phys. Rev. A **76**, 042319 (2007).

[14] G. Wendin, Rep. Prog. Phys. **80**, 106001 (2017).

[15] A. Wallraff, D. I. Schuster, A. Blais, L. Frunzio, R.-S. Huang, J. Majer, S. Kumar, S. M. Girvin, and R. J. Schoelkopf, Nature (London) **431**, 162 (2004).

[16] E. Il'ichev, N. Oukhanski, A. Izmalkov, T. Wagner, M. Grajcar, H.-G. Meyer, A. Y. Smirnov, A. Maassen van den Brink, M. H. S. Amin, and A. M. Zagoskin, Phys. Rev. Lett. **91**, 097906 (2003).

[17] I.-C. Hoi, C. M. Wilson, G. Johansson, J. Lindkvist, B. Peropadre, T. Palomaki, and P. Delsing, New J. Phys. **15**, 025011 (2013).

[18] A. L. Rakhmanov, A. M. Zagoskin, S. Savel'ev, and F. Nori, Phys. Rev. B **77**, 144507 (2008).

[19] A. Zagoskin, A. Rakhmanov, S. Savel'ev, and F. Nori, Phys. Status Solidi B **246**, 955 (2009).

[20] S. Savel'ev, A. M. Zagoskin, A. L. Rakhmanov, A. N. Omelyanchouk, Z. Washington, and F. Nori, Phys. Rev. A **85**, 013811 (2012).

[21] Z. Ivić, N. Lazarides, and G. Tsironis, Sci. Rep. **6**, 29374 (2016).

[22] A. L. Grimsmo, B. Royer, J. M. Kreikebaum, Y. Ye, K. O'Brien, I. Siddiqi, and A. Blais, arXiv:2005.06483.

[23] A. M. Zagoskin, R. D. Wilson, M. Everitt, S. Savel'ev, D. R. Gulevich, J. Allen, V. K. Dubrovich, and E. Il'ichev, Sci. Rep. **3**, 3464 (2013).

[24] V. Giovannetti, S. Lloyd, and L. Maccone, Phys. Rev. Lett. **96**, 010401 (2006).

[25] V. Giovannetti, S. Lloyd, and L. Maccone, Science **306**, 1330 (2004).

[26] A. R. Shlyakhov, V. V. Zemlyanov, M. V. Suslov, A. V. Lebedev, G. S. Paraoanu, G. B. Lesovik, and G. Blatter, Phys. Rev. A **97**, 022115 (2018).

[27] S. Danilin, A. V. Lebedev, A. Vepsäläinen, G. B. Lesovik, G. Blatter, and G. S. Paraoanu, npj Quantum Inf. **4**, 29 (2018).

[28] A. Sørensen, L.-M. Duan, J. I. Cirac, and P. Zoller, Nature (London) **409**, 63 (2001).

[29] A. André and M. D. Lukin, Phys. Rev. A **65**, 053819 (2002).